KFK-522

KERNFORSCHUNGSZENTRUM

KARLSRUHE

Januar 1967

KFK 522

Institut für Neutronenphysik und Reaktortechnik

Investigation of Prompt Neutron Kinetics in the Fast-Thermal Argonaut-Reactor STARK by Noise Analysis

M. Edelmann, T.E. Murley, D. Stegemann

GESELLSCHAFT FÜR KERNFORSCHUNG M. B. H.

KARLSRUHE

KERNFORSCHUNGSZENTRUM KARLSRUHE

Januar 1967 KFK 522

Institut für Neutronenphysik und Reaktortechnik

INVESTIGATION OF PROMPT NEUTRON KINETICS IN THE FAST-THERMAL ARGONAUT-REACTOR STARK BY NOISE ANALYSIS *

M. Edelmann, T.E. Murley, D. Stegemann

Paper presented at the National Topical Conference on
"Coupled Reactor Kinetics"
to be held at Texas A. and M. University (Texas)
23 and 24 January 1967

* Work performed within the association in the field of fast reactors between the European Atomic Energy Community and Gesellschaft für Kernforschung m.b.H., Karlsruhe

Gesellschaft für Kernforschung m.b.H., Karlsruhe

INVESTIGATION OF PROMPT NEUTRON KINETICS IN THE FAST-THERMAL ARGONAUT-REACTOR STARK BY NOISE ANALYSIS

M.Edelmann, T.E.Murley, D.Stegemann

ABSTRACT

As one of a series of experiments using the Fast-Thermal Argonaut-Reactor STARK, investigations were made to study the prompt neutron kinetic behaviour of the coupled system. Assembly 4 was chosen, because it had the highest power fraction in the fast zone permitted by safety considerations. However, even with a power fraction in the fast zone of 31% the coupling between the fast core and the annular thermal driver region was found to be very strong.

A theoretical method for investigating coupled systems is described. It is essentially a modal expansion of the flux which permits a rigorous treatment, within the limits of multigroup diffusion theory, of the space and energy dependence of the prompt neutron flux as well as the location and spectral sensitivity of the neutron detectors. The fundamental, or asymptotic, decay mode and the important higher modes were found, and the calculated decay of prompt neutron chains was compared with that measured by noise techniques.

The experimental techniques applied for these investigations were the Rossi-α method and the probability distribution analysis. A description of the electronic systems is given including improvements regarding the logic circuitry of Rossi-α analyzers. Measurements have been performed in both the fast and thermal regions at various states of reactivity between 0.1 and 4 dollars subcritical. Detectors used in the fast core were ^{3}He-filled proportional counters, and those in the thermal zone were several BF_3-counters distributed symmetrically.

Since the fast and thermal zones were very strongly coupled in this system, the theory did not predict and the measurements did not observe a single dominant fast decay mode attributable to the fast zone, but rather a transient response consisting of a few higher decay modes plus the asymptotic decay mode. In addition, the calculations predicted, and the measurements confirmed, that only the fundamental mode will be found with the detectors placed in the thermal zone, but that a few higher mode transients are observed in the signal with the detectors placed in the fast zone. The calculated and measured asymptotic decay constants agreed well. However, the quantitative comparison of the calculated and measured transient part of the signal is affected by the statistical inaccuracies due to the shortage of experimental data.

I. INTRODUCTION

The zero-power facility STARK is a flexible fast-thermal reactor consisting of a subcritical fast core and a surrounding Argonaut-type thermal driver zone. The basic concept of the system [1] dates back to 1962 when it was recognized that a flexible source reactor would be needed. Therefore, it was decided to convert the Argonaut-Reactor at Karlsruhe into a coupled fast-thermal assembly. The underlying safety philosophy was such that the safety characteristics of the modified reactor with the fast zone still correspond to those of an all-thermal system. Due to this, only moderate fast-core power contributions ($\lesssim$ 40%) can be planned.

The experimental program performed on STARK has two major items:

(a) Development of experimental techniques for investigating fast zero power systems, especially fast reactor mock-ups on the large plutonium-fuelled critical assembly SNEAK.

(b) Investigation of the reactor physics properties of the coupled system STARK and comparison of experimental and calculated data.

Meanwhile, several different fast core loadings have been investigated in STARK containing up to 107 kg ^{235}U in the fast section. A number of experimental and theoretical results concerning spatial distributions of reaction rates, differential neutron spectra, reactivity worths of samples, etc. have been summarized and evaluated in [2]. Also special consideration has been given all the time to determine the kinetic parameters of the coupled system STARK. Three different noise analysis techniques, together with the pulsed source method, have been developed and applied as described in [3].

This paper, in particular, deals with theoretical and experimental results of Assembly 4, which had the highest power fraction in the fast zone (31%) permitted by safety considerations. This paper is thought to contribute a certain aspect to the rather complicated analysis of space- and energy dependent neutron kinetics in the frame of possibilities offered by the fast-thermal system STARK.

II. GENERAL THEORY

A. Rossi-α Technique

The Rossi-α experiment belongs to a class of correlation experiments which is shown schematically in Figure 1 . Two independent neutron detectors monitor a low-power, chain-reacting assembly having an average neutron flux

distribution $\phi_o(x,E)$. The pulses from each detector are passed through separate electronic networks, the first having the impulse response function,

$$a_1(t) = \delta(t - \tau) ,$$

where τ is the delay time of the first network, and since the second network is missing, the second impulse response function is simply

$$a_2(t) = \delta(t) .$$

The resulting signals, $r_1(t)$ and $r_2(t)$, having time-averaged values denoted by $\overline{r_1}$ and $\overline{r_2}$, are multiplied together by a further electronic network. The time-averaged value of the product $r_1(t) \cdot r_2(t)$ is

$$\overline{r_1 \cdot r_2} = \lim_{T \to \infty} \frac{1}{T} \int_0^T r_1(t) \cdot r_2(t) \, dt , \qquad (1)$$

and the correlation function is defined as the difference

$$r_{12}(\tau) = \overline{r_1 \cdot r_2} - \overline{r_1} \cdot \overline{r_2} , \qquad (2)$$

where τ is the delay time.

A general theory has been developed by BORGWALDT and SANITZ [4] to describe the correlation of pulses from two neutron detectors in a reactor. They use a formulation of first collision theory which makes possible the exact treatment of the space- and energy-dependence of the neutron flux as well as the consistent inclusion of detector characteristics and their contribution to the pulse correlation. The general theory was applied in a previous paper [5] to illustrate how one might analyze a Rossi-α experiment in moderator-reflected fast assemblies, and we shall follow closely the notation of Ref. [5].

To briefly outline the mathematical formalism, we consider the kinetic Boltzmann equation using the diffusion approximation and considering only prompt neutrons,

$$B \, \phi(x,E,t) = \frac{1}{v} \cdot \frac{\delta \phi(x,E,t)}{\delta t} , \qquad (3)$$

with associated boundary conditions on the boundary X,

$$\phi(X,E,t) = 0 . \qquad (4)$$

We assume a solution of the form,

$$\phi(x,E,t) = \sum_{n=1}^{\infty} C_n \phi_n(x,E)\, e^{\alpha_n t} , \qquad (5)$$

where the α_n are the eigenvalues and ϕ_n are eigenfunctions of the equation,

$$(B - \frac{\alpha_n}{v})\, \phi_n(x,E) = 0 . \qquad (6)$$

The associated adjoint eigenfunctions are solutions of the adjoint equation

$$(B^+ - \frac{\alpha_m}{v})\phi_m^+(x,E) = 0 , \qquad (7)$$

where the adjoint Boltzmann operator is defined by the usual relation

$$\int_V dV \int_0^{\infty} dE \left[\phi^+ \cdot B\,\phi - \phi \cdot B^+ \phi^+\right] + \text{Boundary Terms} = 0 . \qquad (8)$$

The boundary conditions for ϕ_n^+ are chosen to make the Boundary Terms in Eq.(8) equal to zero.

Multiplying Eq.(6) by $\phi_m^+(x,E)$ and Eq.(7) by $\phi_n(x,E)$ and integrating, we find

$$\int_V dV \int_0^{\infty} dE\, \phi_m^+ \cdot B\, \phi_n - \int_V dV \int_0^{\infty} dE\, \phi_m^+ \cdot \frac{\alpha_n}{v}\, \phi_n = 0 , \qquad (9)$$

and

$$\int_V dV \int_0^{\infty} dE\, \phi_n \cdot B^+ \phi_m^+ - \int_V dV \int_0^{\infty} dE\, \phi_n \cdot \frac{\alpha_m}{v}\, \phi_m^+ = 0 . \qquad (10)$$

The first terms of Eqs.(9) and (10) are equal from Eq.(8), and we deduce the orthogonality relations,

$$\int_V dV \int_0^{\infty} dE\, \phi_m^+ \cdot \frac{1}{v} \cdot \phi_n = \begin{cases} 0 & \text{if } m \neq n \\ V_n & \text{if } m = n . \end{cases} \qquad (11)$$

The normalization constant V_n depends on the normalization scheme of the computer code.

In an earlier paper [5] it was shown that the correlation function can be written as a sum of exponential terms,

$$r_{12}(t) = \sum_{n=1}^{\infty} A_n\, e^{\alpha_n t} , \qquad (12)$$

where the coefficients A_n are calculated from

$$A_n = \left[\int_V dV \int_0^\infty dE\ \sigma_1(x,E)\ \psi_n(x,E) \right] \cdot \left[\int_V dV \int_0^\infty dE\ \sigma_2(x,E)\ \phi_n(x,E) \right] . \quad (13)$$

The cross sections, $\sigma_1(x,E)$ and $\sigma_2(x,E)$, refer to the first and second detector, $\phi_n(x,E)$ is the n^{th} eigenfunction, and $\psi_n(x,E)$ was shown earlier to be the solution of a modified, inhomogeneous Boltzmann equation,

$$(B + \frac{\alpha_n}{v})\ \psi_n(x,E) + \frac{1}{V_n} \cdot \chi(E) \cdot Q_2(x) \cdot f_n^+(x) = 0 . \quad (14)$$

V_n is the normalization constant from Eq.(11) and $\chi(E)$ is the spectrum of prompt fission neutrons. $Q_2(x)$ is the source of neutron pairs at the point x in the stationary system,

$$Q_2(x) = \int_0^\infty dE\ \overline{\nu(\nu-1)}_p \cdot \Sigma_f(x,E)\ \phi_o(x,E) , \quad (15)$$

where $\overline{\nu(\nu-1)}_p$ is the second moment of the prompt fission neutron distribution. The term $f_n^+(x)$ in Eq.(14) is the adjoint source distribution of the n^{th} mode,

$$f_n^+(x) = \int_0^\infty dE\ \chi(E)\ \phi_n^+(x,E) . \quad (16)$$

The calculated correlation function for the Rossi-α experiment is thus represented by the sum of decaying exponential modes given in Eq.(12). In a N-group multigroup calculation with M spatial mesh points, there will be (N·M) separate eigenfunctions. In principle, one must find all of the α's and the coefficients A_n in order to correctly represent the measured correlation function, since recent measurements have shown that the prompt-neutron chains in reflected fast reactor assemblies decay with modes other than the fundamental mode [6]. In practice, however, it is necessary to find only the lowest few α's, since the many modes with very large negative decay constants will make only a very small contribution to the measured signal.

Since all of the measurements were made on systems which were sub-prompt critical, all of the α's are negative. The eigenvalue of largest algebraic value is α_1, and the corresponding fundamental mode eigenfunction, $\phi_1(x,E)$,

is everywhere positive in the reactor.* The eigenvalue calculation is simply a trial-and-error search to find how much pseudo-absorption, α_n/v, must be added uniformly to the system in order to preserve the neutron balance at each energy and at each spatial point for the n^{th} mode. Since $\alpha_n < 0$, we are effectively subtracting a uniform 1/v-absorber, and the higher mode spectra thus become softer with increasing negative α_n. In fact, the effective absorption cross section, $\Sigma_a(E) + \alpha_n/v(E)$, must be negative in certain regions of the system for the n^{th} higher mode. In order to preserve the neutron balance for all spatial points, the low-energy flux in the n^{th} mode must be negative in that region. Hence, we see that the higher modes are characterized by eigenfunctions showing strong fluctuations in space and energy.

The Rossi-α experiment measures the time decay of fission-chain-related neutrons in the system following the detection of a single neutron from the same chain. These chain-related neutrons will, for the average of many chains, have a spatial and energy distribution that is not too different from the total flux distribution. Thus, one would expect that the correlation function, $r_{12}(t)$, in Eq.(12) could be adequately represented by the fundamental mode plus a very few of the next higher modes. We shall see in section VI that this is the case for the measurements in STARK.

B. Analysis of Probability Distributions

The direct analysis of probability distributions allows an easy and appropriate way to compute variance over mean values. The application of this technique for the analysis of neutronic noise has already been treated in [8,3]. If the distribution of probabilities $p_n(T)$ for registering n counts in specified time intervals of variable length T can be directly measured, the average $\bar{n}(T)$, the variance $\overline{n^2}(T) - \bar{n}^2(T)$, and the quantity $\left[\overline{n(n-1)}(T) - \bar{n}^2(T)\right]$ can be easily calculated by the following equations:

---

* We deal here with systems near enough to critical ($k \geq 0.8$) that an asymptotic decay mode can indeed be observed. Furthermore, we assume that the energy group structure is well chosen, such that the asymptotic decay mode corresponds to the everywhere-positive fundamental mode. The exceptional cases where these conditions are not met are discussed by STORRER [7].

$$\bar{n}(T) = \sum_{n=1}^{\infty} p_n(T)\, n \qquad (17)$$

$$\overline{n^2}(T) = \sum_{n=1}^{\infty} p_n(T)\, n^2 \qquad (18)$$

$$\overline{n(n-1)}(T) - \bar{n}^2(T) = \sum_{n=2}^{\infty} p_n(T)\, n(n-1) - \left[\sum_{n=1}^{\infty} p_n(T)\, n\right]^2 . \qquad (19)$$

The relation between the above quantities and the reactor physics parameters using the point reactor model is wellknown and discussed in [8]. An extension of this work within the space- and energy-dependent treatment leads to:

$$Y(T) = \frac{\overline{n(n-1)}(T) - \bar{n}^2(T)}{\bar{n}(T)} = \frac{2}{\bar{r}} \sum_n \frac{A_n}{\alpha_n} \left(1 - \frac{1 - e^{-\alpha_n T}}{\alpha_n T}\right), \qquad (20)$$

where the α_n are the eigenvalues of Eq.(6), and the coefficients A_n are calculated from Eq.(13).

III. NUMERICAL PROCEDURE

The numerical evaluation of the foregoing equations is accomplished using the flexible, one-dimensional multigroup diffusion code of the Karlsruhe Nuclear Program System, NUSYS [9], which has been written in FORTRAN II for a 10 K version of the IBM 7074. Basic input data for the code are geometry parameters and material compositions of all reactor zones. The group constants of the 26-group set of ABAGJAN, et al. [10] were used.

A. Radius Iteration

In the first phase we calculate the dimensions or material compositions necessary to achieve a prescribed k_{eff}, in this case $k_{eff} = 1 - \beta_{eff}$. The output of this stage are the exact dimensions of the system, the stationary neutron flux, $\phi_o(x,E)$, the stationary adjoint flux, $\phi_o^+(x,E)$, and the fission neutron source, which as a good approximation is assumed to be proportional to the binary source $Q_2(x)$.

$$Q_2(x) \sim \int_0^{\infty} dE\ \nu(x,E)\ \Sigma_f(x,E)\ \phi_o(x,E) . \qquad (21)$$

B. Search for Eigenvalues α_n

The asymptotic prompt-neutron decay constant, α_1 , is the most important single quantity measured in the experiments, and it is necessary to calculate it using the full 26-group structure. In this phase Eqs.(6) and (7) are solved for the lowest mode using an iterative algorithm. An input option allows one to specify the prompt ν's for the i^{th} fissionable isotope by the relation,

$$\nu^i_{prompt} = \nu^i (1 - \beta^i) , \qquad (22)$$

where β^i is the delayed neutron fraction of the i^{th} fissionable isotope (11).

An estimate and a tolerance are given for α_1 ; using this estimate a pseudo-absorption term α_1/v is introduced into all zones, and $k_{prompt} = k(\alpha)$ is calculated. If $k \neq 1$, the difference $k - 1$ and the associated flux and adjoint functions are inserted into a perturbation functional to improve the estimate of α_1 . This iteration proceeds until $k = 1.0$. The output of this stage are the eigenvalue, α_1 , the eigenfunction and adjoint function, $\phi_1(x,E)$ and $\phi_1^+(x,E)$, the fission-spectrum-weighted adjoint source, $f_1^+(x)$, and the normalization constant V_1 .

The same procedure is followed for finding the higher modes having negative flux components. As mentioned earlier, the number of eigenvalues is equal to the group number times the meshpoint number. The higher eigenvalues are closely spaced in a 26-group calculation, and the computation time for the α-searches is therefore very great. Since the non-asymptotic part of the correlation function is being approximated by a sum of higher mode exponential terms, we assume that the transient part of the signal can be described adequately using a few exponential terms calculated in a 4-group α-search. The cross sections are collapsed from 26-groups to 4-groups using the stationary flux $\phi_o(x,E)$ as the weighting spectrum. In the calculations for Assembly 4 of **STARK**, both the critical mass and the lowest eigenvalue were found to be within 20% of those from the 26-group calculation, indicating that the cross section reduction did not seriously distort the description of the system.

C. Inhomogeneous Calculation

In this phase we calculate $\psi_n(x,E)$ for each mode by solving Eq.(14). As input we use the prompt ν's of Eq.(22), the binary source $Q_2(x)$, the adjoint source $f_n^+(x)$, and the normalization factor V_n. We also note that in the calculation of $\psi_n(x,E)$ we are adding the pseudo-1/v absorber instead of subtracting it as in the calculation of $\phi_n(x,E)$. The final step is to compute the coefficients A_n from Eq.(13).

IV. EXPERIMENTAL TECHNIQUES

A. Rossi-α Technique

During the first Rossi-α experiments performed on STARK [3] it was found that the analyzer systems used so far mainly in fast reactors are not directly applicable to thermal systems. More generally expressed, this means that conventional time analyzers are not adequate if the counting rate of the detector pulses triggering the analyzer is almost equal or larger than the α-value to be measured. Discrepancies between theory and experiment due to this have been reported also by other authors [13,14].

To analyze these effects in more detail theoretical and experimental investigations have been made at Karlsruhe by BORGWALDT [15] and EDELMANN [16]. Because the results are conclusive for the proper application of the Rossi-α method a short summary will be given in this context. The discrepancies found between theory and experiment are due to deadtime losses in the analyzer so far not considered in theoretical derivations. The model taking into account deadtime effects shows that the amplitude of the correlation function is seriously affected by dead time losses. The conclusion is that all pulses of the trigger-channel have to be used to start the analyzer for a proper Rossi-α experiment. There are two possible ways for this:

(a) Reduction of counting rate in the trigger channel. This leads obviously to an increase in measuring time, but the results are much better than with high counting rates and large deadtime losses because the signal-to-background ratio is increased.

(b) Development of an "deadtime-free" time analyzer, which can handle counting rates higher than the values of prompt neutron decay constants to be measured.

The second more advantageous solution has been chosen especially in view of investigations planned in large plutonium fuelled fast assemblies.

The new time analyzer developed is in principle a very flexible and versatile digital version of the delayed coincidence analyzer used by ORNDOFF (17), which is shown in Figure 3. In the ORNDOFF-analyzer the trigger pulses are delayed by a number of ten delay lines from which they are fed into coincidence counting channels. In our case, 32 time channels seemed to be necessary at minimum. A digital 132 stage shift register* and a 4 MC crystal oszillator with frequency divider is used instead of the delay lines and the gate generator. A time channel of the analyzer is formed by different numbers of stages - selectable by a switch - together with a coincidence circuit and scaler. The channel width can be chosen between 0.25 and 1024 microseconds.

For better time resolution of the fast transient part of the prompt neutron response curves a special feature of the analyzer is the possibility to use shorter widths in the first nine channels and larger ones in the rest of the time cycle. The mean deadtime for starting analysis cycles is equal to the largest channel width being used in the experiment.

The contents of the scalers scaling the coincidence pulses are read out on a paper-tape perforator and on a type writer. The data are automatically evaluated by a least-squares fit program.

B. Analysis of Probability Distributions

For the measurement of the probabilities $p_n(T)$ an experimental set-up was built, where n can range from 0 to 127. This probability distribution analyzer is schematically shown in Figure 2. Because a detailed description of the apparatus, including automatic control and data acquisition and reduction system, has been given elsewhere (12) it will be mentioned only briefly here. The operating principle is as follows: Pulses from one or more detectors are fed into the input A of a fast acting electronic step switch, which proceeds by one step for each incoming pulse. Pulses from a time marker terminating the length T of the time interval are fed into input B. According to the position of the electronic switch a gate is opened for the time pulse, which gives a signal to the scaler connected to this output. If, for instance,

* Manufactured by Borer and Co., Solothurn, Switzerland.

4 counts came in during the interval, output 4 of the switch opens gate 4 so that the pulse from the time marker delivers a signal into scaler 4. That means, that 4 counts came in during this time interval. The step switch is reset and the probability distribution analyzer is opened for a new cycle. After a sufficiently long time the run for one T-value is finished and the probabilities $p_n(T)$ are obtained by dividing the number of counts in scaler n, R_n, by the number of counts in the time interval scaler, R_T, giving

$$p_n = \frac{R_n}{R_T} \quad .$$

The computation of the average, the variance etc., according to Eqs.(17-20) is then straight-forward.

V. MEASUREMENTS

The measurements have been performed in Assembly 4 of STARK. The basic geometrical structure of STARK including the detector positions used is shown in Figure 4. The fast core (37.2 cm average diameter) is formed by an array of 37 vertical stainless-steel matrix tubes which are fixed by a bottom grid plate. The tubes are filled with platelets (5.1 by 5.1 cm) of various core materials. In order to prevent strong peaks in the ^{235}U-fission rate at the edge of the fast zone, the core structure is enclosed in a 5 cm-thick natural uranium casing which absorbs slow neutrons incident from the outer driver zone. Thus, coupling between the zones is maintained mainly by the exchange of fast neutrons.

The thermal core consists of conventional Argonaut type fuel plates and light water as a moderator. The fuel plates, each of them containing 20.83 g ^{235}U (20 percent enriched), are arranged in 24 groups with a 6.3 mm spacing inside an annular aluminium tank; the volume between the fuel region and the outer tank wall is filled with graphite plates and wedges.

The material composition of STARK, Assembly 4, is given in Table I. Also other characteristic data as fuel masses and power contributions of the different zones are included in Table I for illustration.

Detectors used for measurements in the fast core were ^{3}He-filled proportional counters because of the relatively large cross section of ^{3}He for fast neutrons and the high filling pressure possible. A bundle of four specially designed fast ^{3}He counting tubes (Texas Nuclear Corporation) connected in

parallel with 0.625 inch diameter and 12 inches sensitive length each, having a filling pressure of 10 atmospheres, were placed in position 19 at the center of the fast zone as indicated in Figure 4. In the thermal zone four BF_3-proportional counters, distributed symmetrically around the annular thermal core as shown in Figure 4, were connected in parallel for these experiments. By this arrangement higher spatial harmonics due to asymmetry and azimuthal excitation are suppressed.

Although measurements have been performed in both the fast and thermal regions at various states of reactivity between 0.1 and 4 $ subcritical, only the results at 1 $ subcritical have been chosen as representative examples for comparison with theory.

Pulses from the detectors in the fast and thermal zone have been recorded on magnetic tape by use of an AMPEX FR 1300 tape recorder. One reason for this procedure was the utilization of the same detector pulses for the analysis by both the Rossi-α method and the probability distribution technique. Furthermore, the same pulses could be used for auto- and crosscorrelation measurements.

VI. RESULTS FROM THEORY AND EXPERIMENTS

As main reference point to compare theory and experiment a reactivity state of 1 $ subcritical was chosen, because measurements at delayed critical were not possible due to the inherent source strength of about $2 \cdot 10^4$ neutrons per sec produced by spontaneous fissions in the natural uranium buffer zone. Further, it was found from theoretical calculations that the coefficients A_n $(n > 1)$ are larger at 1 $ subcritical than at delayed critical. The calculations were carried out according to the steps outlined in Section III. The calculated and measured asymptotic decay constants for 1 $ subcritical agreed very well:

$$\alpha_1(\text{measured}) = -230\ \text{sec}^{-1} \pm 3\ \text{sec}^{-1}$$
$$\alpha_1(\text{calculated}) = -232\ \text{sec}^{-1} (\pm 9\ \text{sec}^{-1}\ \text{from uncertainties in the}\ \beta^i).$$

In addition, the next three higher eigenvalues were computed in a 4-group calculation to be:

$$\alpha_2 = -1878\ \text{sec}^{-1}$$
$$\alpha_3 = -3949\ \text{sec}^{-1}$$
$$\alpha_4 = -6982\ \text{sec}^{-1}\ .$$

Further α-searches failed to find any more eigenvalues in this range, and the next higher α's seem to be in the vicinity of 20,000 to 30,000 sec^{-1}.

The corresponding eigenfunctions $\phi_n(x,E)$ are shown in Figure 5, where the higher modes are characterized by having nodes only in the thermal energy group. The detector weighting functions $\psi_n(x,E)$ are shown in Figure 6, where we see they are positive everywhere, and the spectrum becomes harder with increasing α_n.

The correlation function measured in the experiments depends on the location and spectral sensitivity of the detectors used. Direct comparisons of experiment and theory were made for autocorrelation in the fast zone with ^3He-detectors and autocorrelation in the thermal zone with BF_3-detectors. The coefficients A_n - see Eq.(13) - calculated for these two cases at 1 $ subcritical are as follows:

Detector locations	α_1=-232 sec^{-1}	α_2=-1878 sec^{-1}	α_3=-3949 sec^{-1}	α_4=-6982 sec^{-1}
I. ^{10}B-detectors at pos. 21,23,25,27	A_1 = 1.000	A_2 = 0.190	A_3 = -0.083	A_4 = -0.086
II. ^3He-detectors at pos. 19	A_1 = 1.000	A_2 = 0.280	A_3 = 0.223	A_4 = 0.065
	sec^{-2}	sec^{-2}	sec^{-2}	sec^{-2}

In the first case the calculation of the higher mode coefficients indicates that these modes tend to cancel and, in fact, the experiment showed no deviation from the fundamental decay mode, as can be clearly seen from the Rossi-α curve shown in Figure 7.

In the second case with fast neutron detectors at the center of the core, the calculations predicted and the Rossi-α measurements confirmed that a few higher mode transients are observed in addition to the asymptotic decay mode. Figure 8 shows the calculated and measured decay of prompt neutrons in the fast core at 1 $ subcritical. We see that the calculated curve is in qualitative agreement with the measured data, showing the contribution of the transient modes for times t ≳ 2 milliseconds. An exact quantitative comparison of the calculated and measured transient part of the signal is not feasible

in this case, because the contribution of the higher modes to the signal is not very large, and because there was only a limited accuracy achievable in this time region.

Furthermore, crosscorrelation experiments using the Rossi-α method have been performed between the fast and thermal core. If the pulses from the detectors in the thermal core are used to trigger the time analyzer and those from the detectors in the fast core are analyzed, the resulting curve does not differ in shape from the one shown in Figure 7 so that only the fundamental decay mode is observed. In the reverse crosscorrelation experiment, where the detector pulses from the fast core trigger the analyzer, a different type of curve is found as shown in Figure 9. A time delay of about 1 millisecond is observable before the prompt decay corresponding to the fundamental mode occurs. The delay is due to the fact that fast neutrons from the fast core acting as source in the thermal zone are slowed down and diffuse before generating new fissions. The analogy between Rossi-α and pulsed source experiments becomes especially evident in this case. The decay constants of the fundamental mode measured in the Rossi-α cross- and autocorrelation experiments at - 1 $ are listed in Table II.

The probability distribution method has also been applied to analyze the same detector pulses stored on magnetic tape as have been used for the Rossi-α measurements. The case II, referred to above, where pulses from ^{3}He-detector in the center of the fast core at 1 $ subcritical were analyzed, is shown in Figure 10. The quantity Y(T) as function of time interval length T as found from the experiment is compared to the theoretical curve calculated according to Eq.(20), using the values for α_n and A_n, which have been listed above for case II. The influence of higher modes in the quantity Y(T) measured by this technique is much weaker than on the corresponding prompt neutron decay curve measured by the Rossi-α method. The reason for this follows from Eq.(20) where the coefficients A_n/α_n decrease with increasing α_n. To illustrate this, the contribution of the second decay mode (A_2, α_2) has been drawn also into Figure 10, using an enlarged scale (x5).

VII. CONCLUSIONS

The results of the investigations of the prompt neutron kinetic behavior of the reactor STARK, Assembly 4, using noise analysis techniques are thought to be a contribution to understanding the kinetic behavior of fast-thermal coupled systems. Since the fast and thermal zones were very strongly coupled

in this system, the theory did not predict and the measurements did not observe a single, dominant fast decay mode attributable to the decay of fission chains in the fast zone, but rather a transient response made up of a few higher modes in addition to the asymptotic decay mode.

An important result of this work is that the problems involved both in improving the experimental techniques and in the theoretical interpretation of the results have now become more clearly defined.

In regard to the experimental techniques it can be concluded that the two noise analysis techniques applied here are a helpful tool for the investigation of coupled reactor kinetics. The Rossi-α technique, in particular, is best suited to measure the fundamental mode and higher transient modes of the prompt neutron decay, if there are few and well separated eigenvalues. In the range where closer spacing of eigenvalues occurs, the attenuation of higher modes in the probability distribution analysis is advantageous to separate the fundamental mode if this is no longer possible by the Rossi-α method. It is, therefore, favourable to combine these two techniques for the investigation of either flexible fast-thermal coupled systems or fast systems with moderating reflectors.

The theory developed by BORGWALDT and SANITZ [4] is applicable to a large class of critical or near-critical reactor systems and for any type and combination of neutron detectors. One may encounter practical difficulties, however, in applying the theory to some fast systems because of the need to retain many energy groups to describe the spectrum adequately. Such a large number of energy groups, in turn, increases the number of higher modes and complicates the search for the higher eigenvalues. Thus, further work should be done to simplify the numerical procedure.

ACKNOWLEDGEMENT

The authors are indebted to Dr. H. BORGWALDT and D. SANITZ for many helpful discussions for improving and applying the computer code. Further, we wish to acknowledge the assistance given by the STARK operation staff, in particular Chr. BRÜCKNER, during the experimental work.

REFERENCES

(1) H.MEISTER, K.H.BECKURTS, W.HÄFELE, W.H.KÖHLER, and K.OTT, "The Karlsruhe Fast-Thermal Argonaut-Reactor, Concept", KFK-217, Kernforschungszentrum Karlsruhe (1964).

(2) L.BARLEON, et al., "Evaluation of Reactor Physics Experiments on the Coupled Fast-Thermal Argonaut-Reactor STARK", KFK-482, Kernforschungszentrum Karlsruhe (1966).

(3) M.EDELMANN, G.KUSSMAUL, H.MEISTER, D.STEGEMANN, and W.VÄTH, "Pulsed Source and Noise Measurements on the STARK Reactor at Karlsruhe", KFK-303 and IAEA-Proceedings on Pulsed Neutron Research, Vol. II, 799-824 (1965).

(4) H.BORGWALDT, D.SANITZ, "Impulskorrelation zweier Neutronendetektoren im stationären Reaktor", Nukleonik, 5, 239-249 (1963).

(5) H.BORGWALDT, T.E.MURLEY, D.SANITZ, "The Modal Synthesis of Rossi-α Data for Moderator-Reflected Fast Assemblies", KFK-409, Kernforschungszentrum Karlsruhe (1966).

(6) G.S.BRUNSON, et al., "A Survey of Prompt-Neutron Lifetimes in Fast Critical Systems", ANL-6681, Argonne National Laboratory (1963).

(7) F.STORRER, "Pulsed Neutron Experiments on Fast and Intermediate Systems", IAEA-Proceedings on Pulsed Neutron Research, Vol.II, 317-336 (1965).

(8) H.BORGWALDT, D.STEGEMANN, "A Common Theory for Neutronic Noise Analysis Experiments in Nuclear Reactors", Nukleonik, 7, 313-325 (1965).

(9) H.BACHMANN, et al., "The Karlsruhe Nuclear Code System NUSYS", to be published.

(10) L.P.ABAGJAN, et al., "Gruppenkonstanten schneller und intermediärer Neutronen für die Berechnung von Kernreaktoren", translated from the Russian as KFK-tr-144, Kernforschungszentrum Karlsruhe (1964).

(11) G.R. KEEPIN, Physics of Nuclear Kinetics, Table 4.14, p.102, Addison-Wesley, Reading, Mass. (1965).

(12) D.STEGEMANN, "Die Analyse des Neutronenrauschens in Reaktoren", Externer Bericht INR-4/66-1, Kernforschungszentrum Karlsruhe (1966).

(13) T.STRIBEL, "Neutronen-Lebensdauer- und Reaktivitätsmessungen an thermischen Reaktoren mit Hilfe der Rossi-α-Methode, Nukleonik, 5, 170-173 (1963).

(14) H.CHRISTENSEN, D.BABALA, T.BERGEM, St.JOVANOVIC, E.STORMARK, W.SUWALSKI, "A Review of Nora Project Noise Experiments", Proc. Int. Symp. on Neutron Noise, Waves, and Pulse Propagation, Gainesville, Florida (1966).

(15) H.BORGWALDT, "Einheitliche Theorie der Korrelationsexperimente in Nullleistungsreaktoren", Externer Bericht INR-4/66-5, Kernforschungszentrum Karlsruhe (1966).

(16) M.EDELMANN, unpublished.

(17) J.D.ORNDOFF, "Prompt Neutron Periods of Metal Critical Assemblies", Nucl. Sci. and Eng. 2, 450-460 (1957).

LIST OF FIGURES AND TABLES

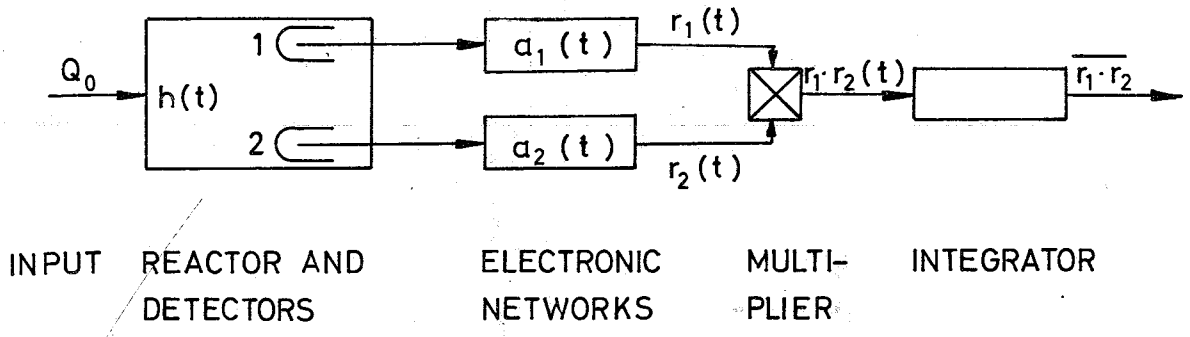

FIG.1 Scheme of a correlation experiment

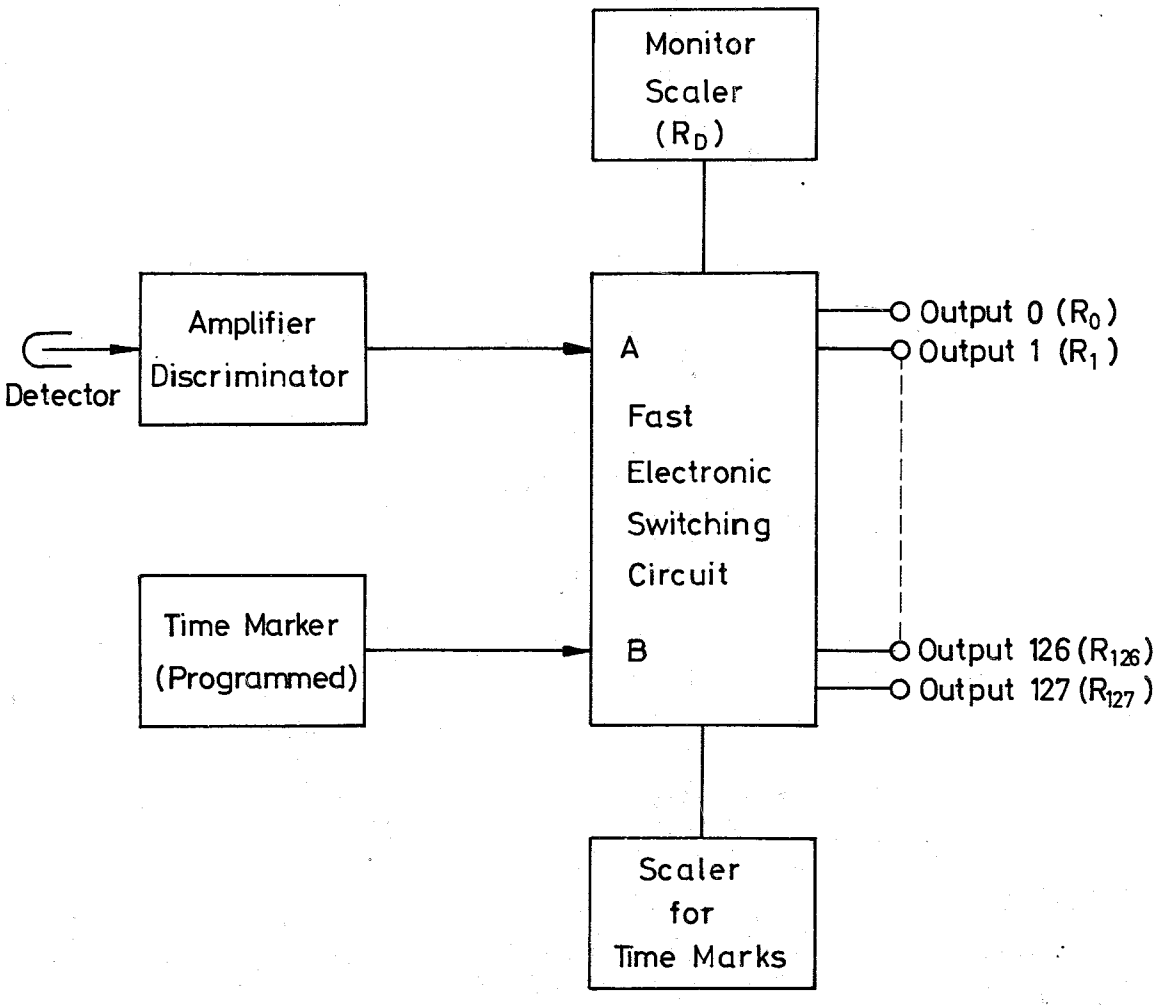

FIG.2 Schematic diagram of probability analyzer

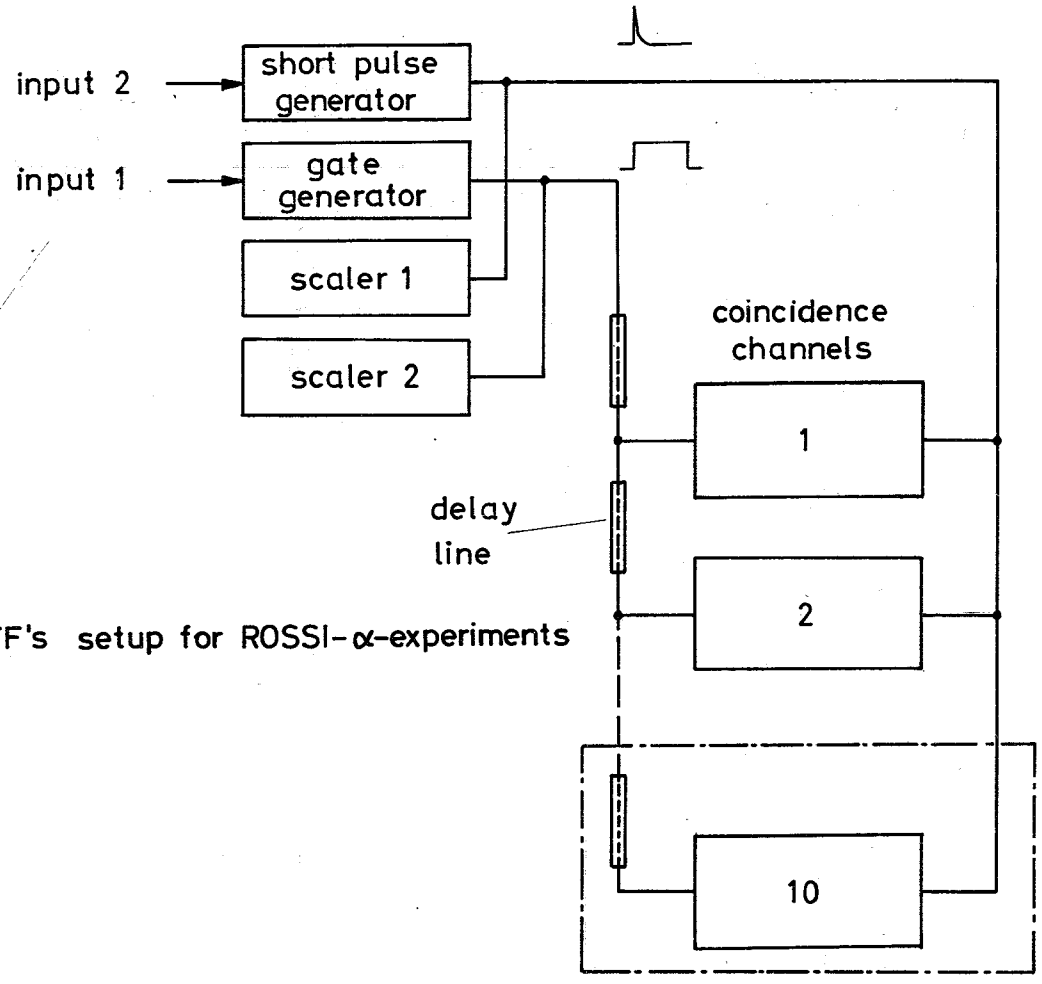

ORNDOFF's setup for ROSSI-α-experiments

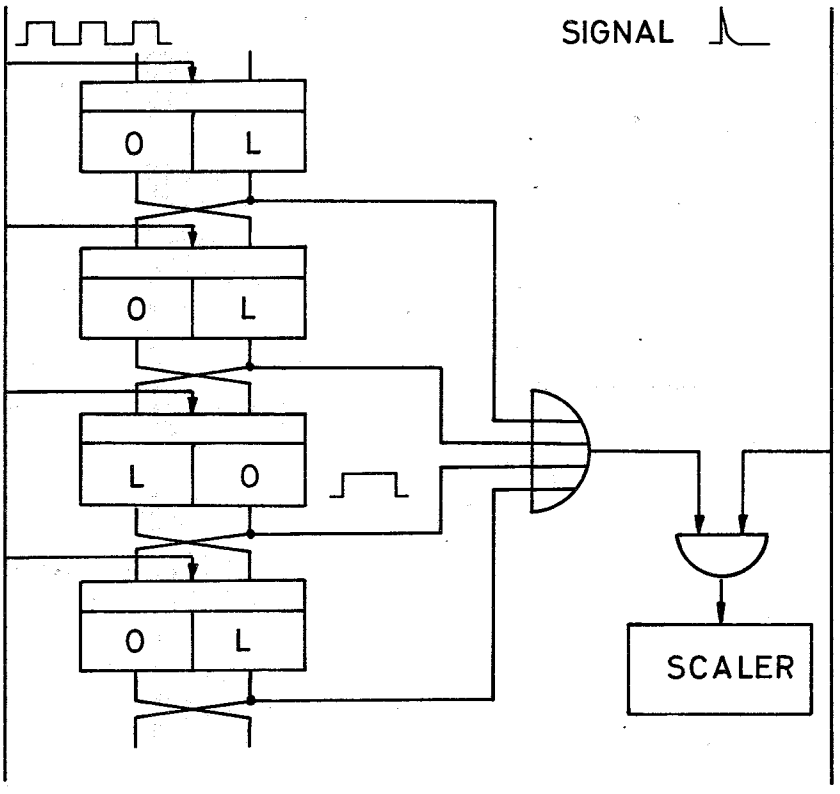

ONE CHANNEL OF THE NEW ANALYZER CON - SISTING OF 4 STAGES (FLIP FLOPS) OF THE SHIFT REGISTER

FIG.3 Set-up for Rossi-α experiments

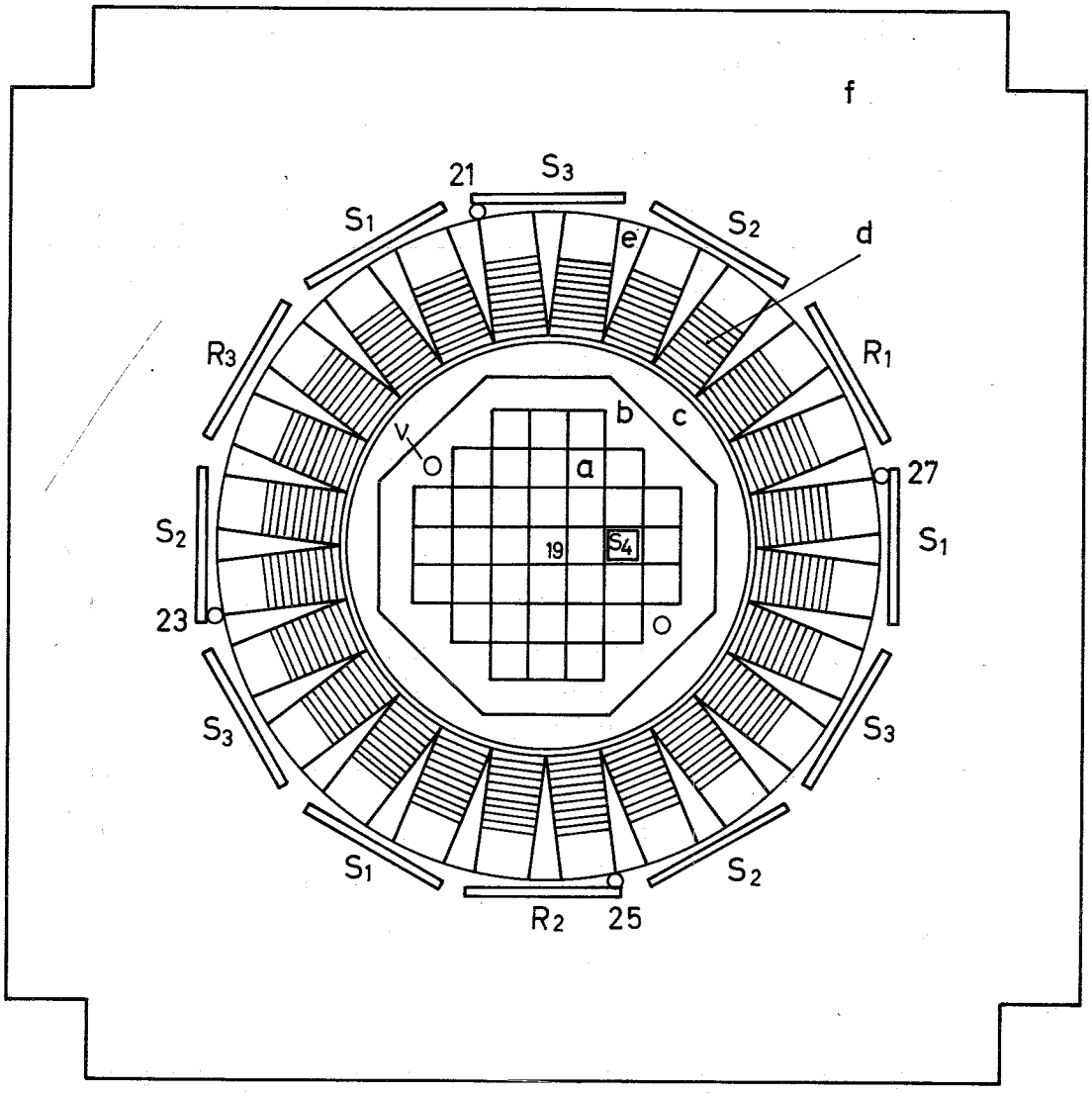

FIG.4 Schematic cross section of STARK

a - fast core
b - natural uranium zone
c - graphite region
d - thermal core (fuel region)
e - thermal core (graphite pieces)
f - graphite reflector
v - vertical channel

R_1, R_2, R_3 - fine-control plates
S_1, S_2, S_3 - safety plates
S_4 - fuel-poison safety rod
19 - position of fast ^{3}He-detectors
○ 21,23,25,27 - positions of $^{10}BF_3$-detectors

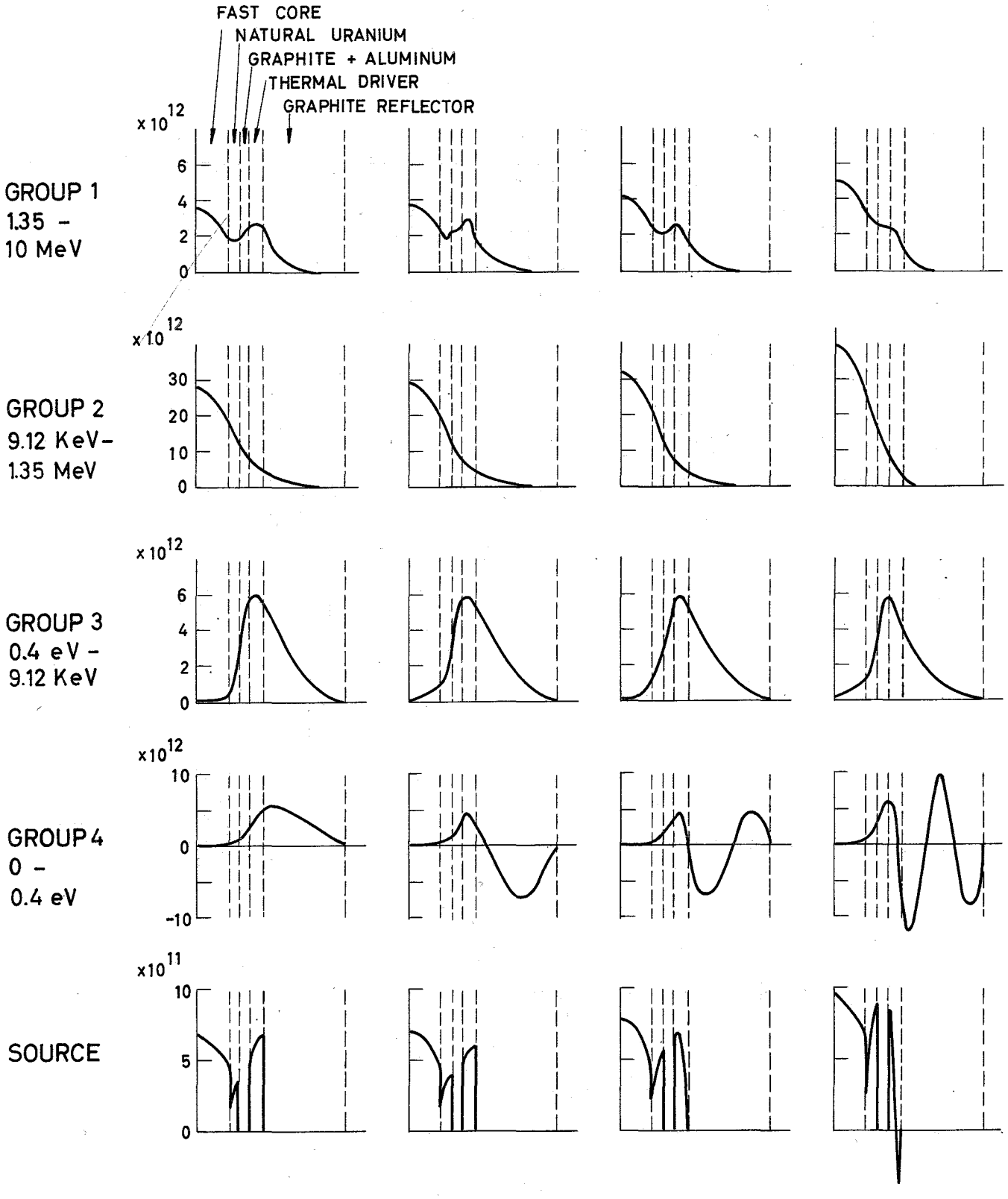

FIG. 5 $\phi_n^i(r)$ vs. r

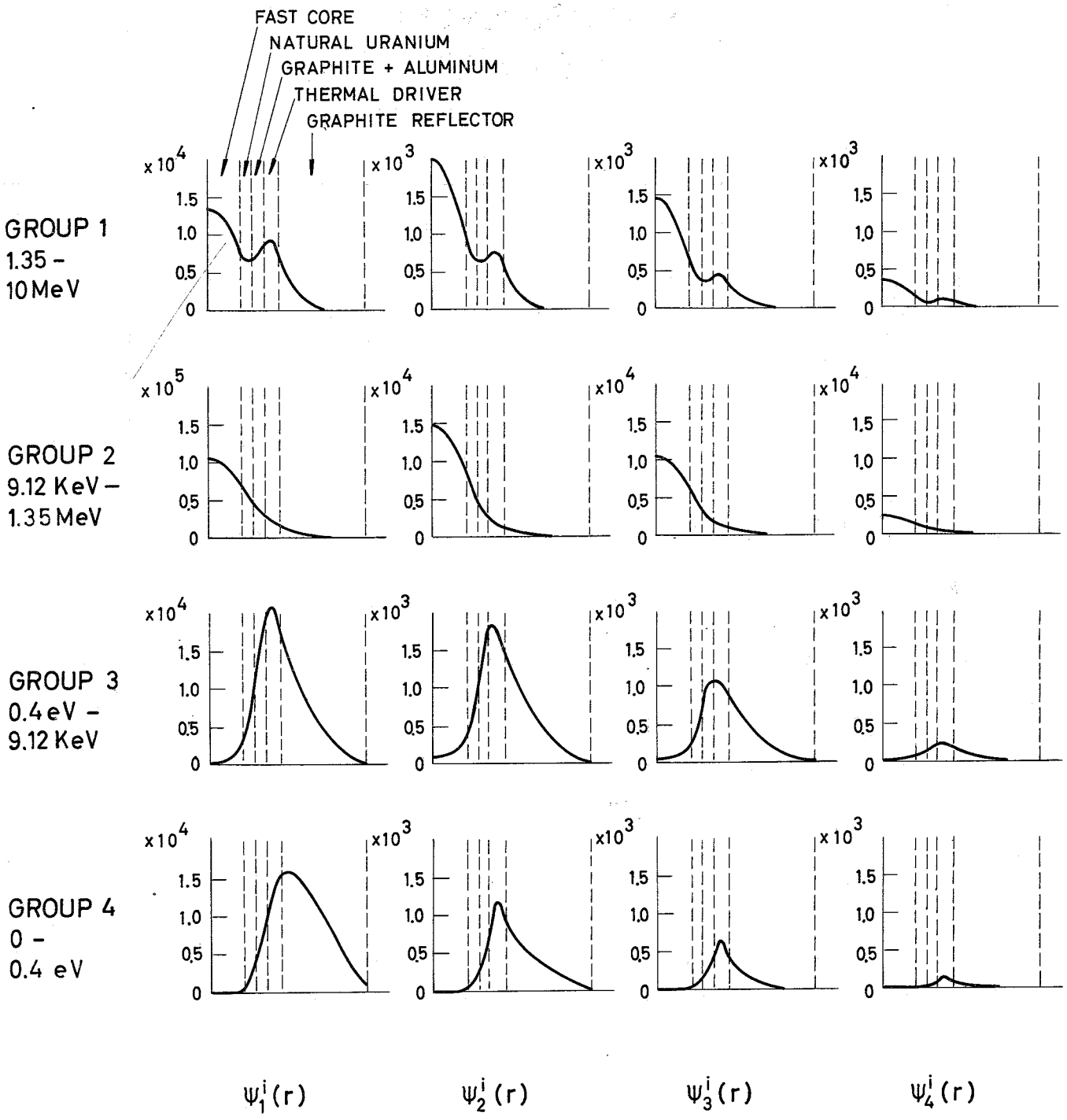

FIG. 6 $\psi_n^i(r)$ vs. r

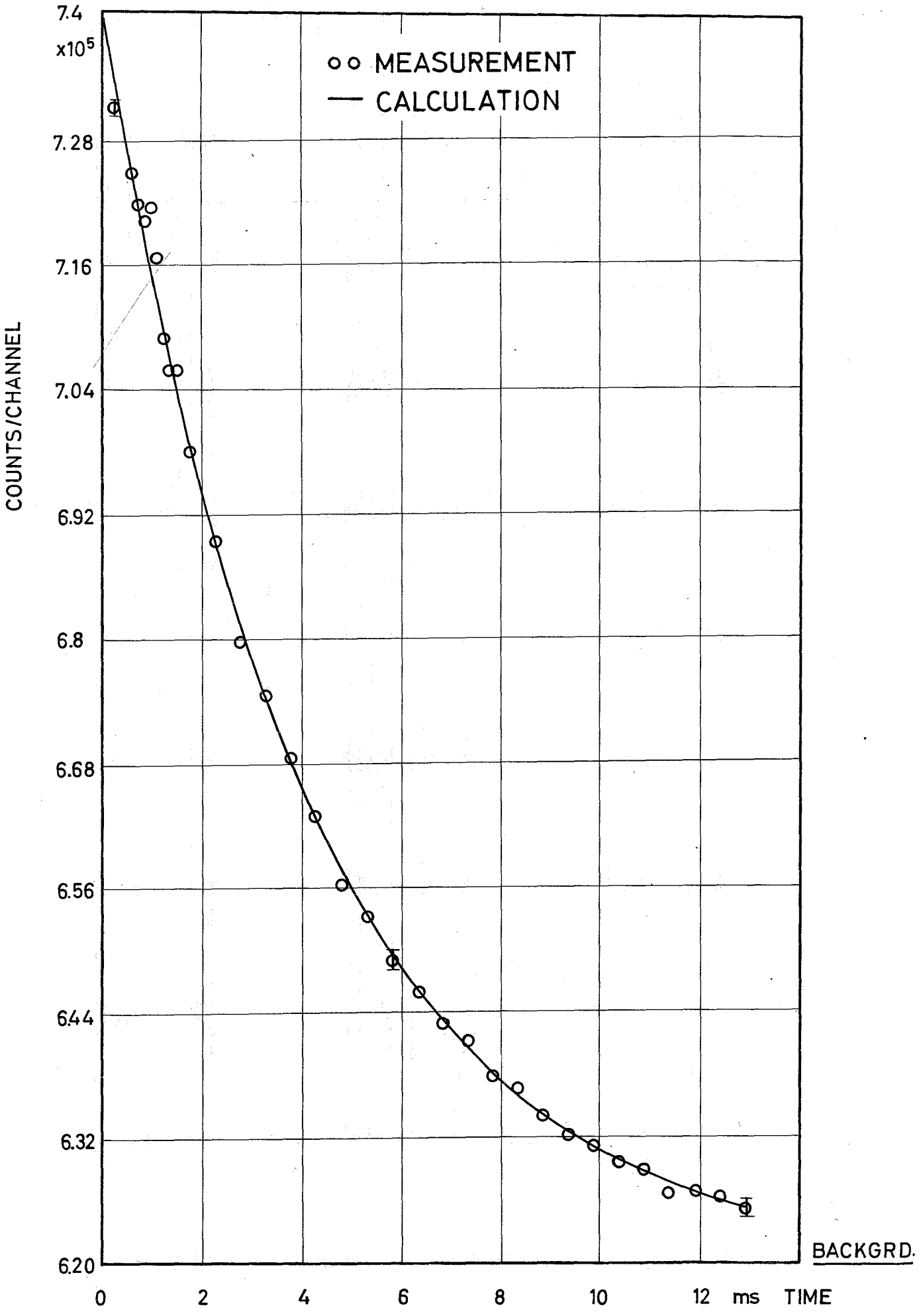

FIG.7 Comparison of calculated and measured prompt neutron decay in Assembly 4 of STARK at 1 $ subcritical (thermal core)

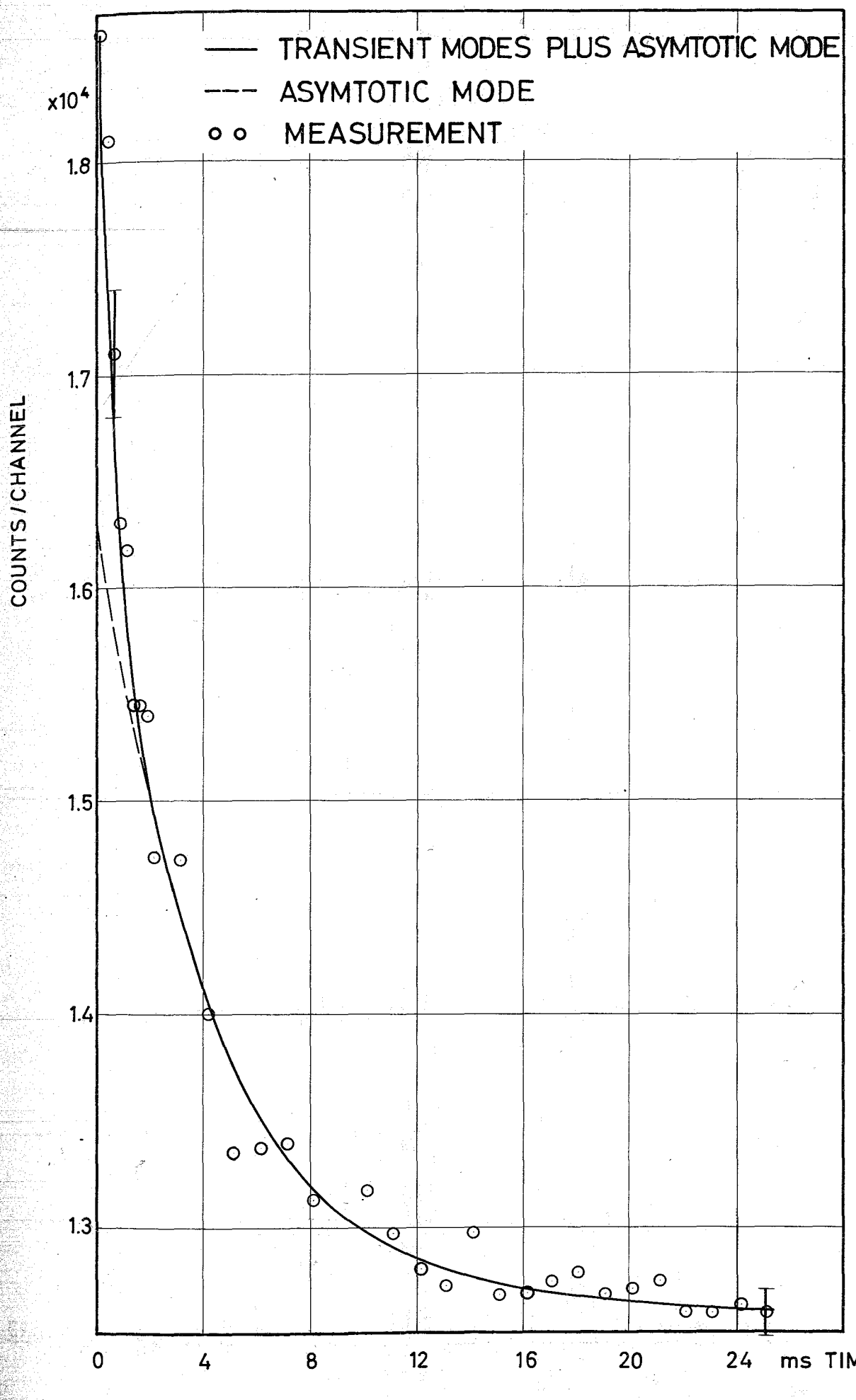

FIG.8 Comparison of calculated and measured prompt neutron decay in Assembly 4 of STARK at 1 $ subcritical

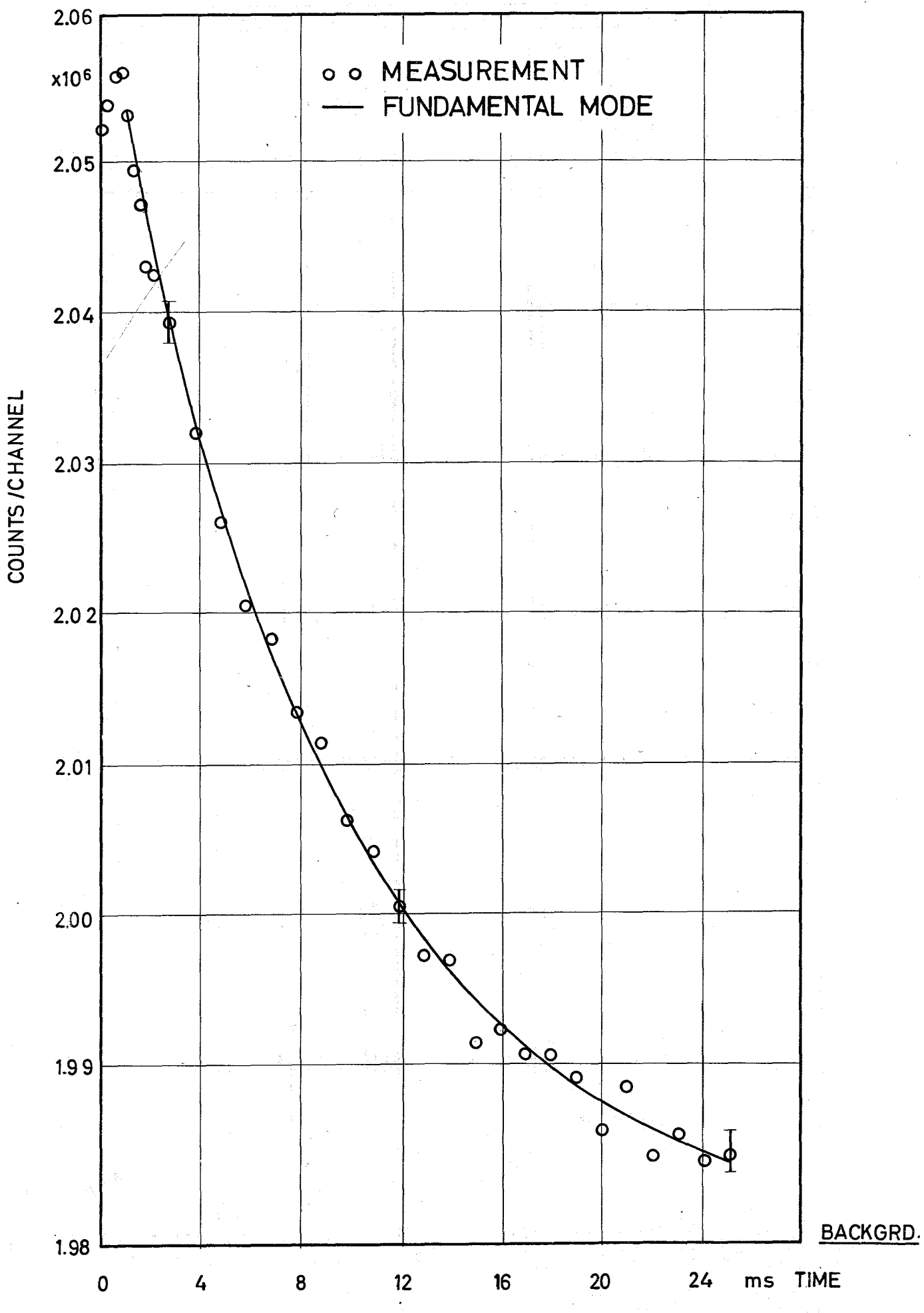

FIG.9 Time behaviour of prompt neutrons from crosscorrelation measurement between fast and thermal core of STARK, Assembly 4

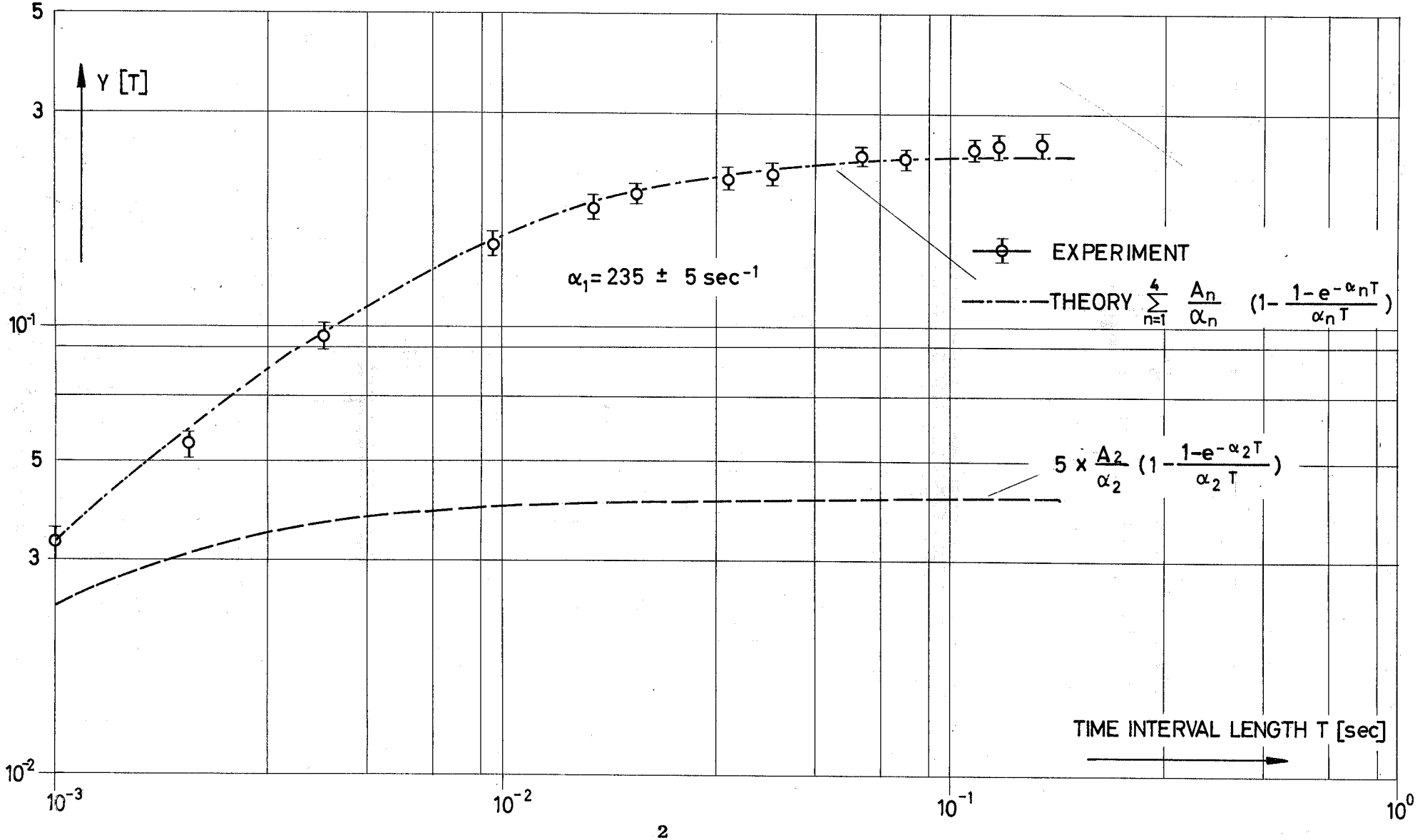

FIG.10 $Y(T) = \frac{\overline{n(n-1)} - \bar{n}^2}{\bar{n}}$ as function of time interval length T

Table I

Material composition (atoms per cm^3) and characteristic data of STARK, Assembly 4

Zone		Fast Core	Natural uranium	Graphite + air gap	Thermal core	Graphite	Graphite + air gap	Graphite reflector
Outer radius		18.6 cm	24.2 cm	30.5 cm	38.5 to 45 cm	46.5 cm	50.5 cm	86.5 cm
Material:								
H - 1				$3.680 \cdot 10^{20}$	$3.726 \cdot 10^{22}$		$2.527 \cdot 10^{20}$	
C - 12				$4.922 \cdot 10^{22}$	$1.468 \cdot 10^{22}$	$8.526 \cdot 10^{22}$	$4.127 \cdot 10^{22}$	$8.526 \cdot 10^{22}$
O - 16		$1.4428 \cdot 10^{22}$			$2.003 \cdot 10^{22}$			
Al - 27		$9.619 \cdot 10^{21}$		$9.264 \cdot 10^{21}$	$1.343 \cdot 10^{22}$		$3.484 \cdot 10^{21}$	
Fe - 56		$6.042 \cdot 10^{21}$						
U - 235		$4.1597 \cdot 10^{21}$	$3.437 \cdot 10^{20}$		$1.0495 \cdot 10^{20}$			
U - 238		$2.6330 \cdot 10^{22}$	$4.739 \cdot 10^{22}$		$4.193 \cdot 10^{20}$			
Fuel mass (kg ^{235}U)	exp.	106.90	9.35		4.43			
	calc.				4.429			
Power contributions (%)	exp.	31.1	10.9		58.0			
	calc.	33.5	11.4		55.1			

Table II

Prompt neutron decay constants of the fundamental mode from Rossi-α measurements performed in fast and thermal core of STARK, Assembly 4 at - 1 $

Position of detector 1	Position of detector 2	α_1 [sec^{-1}]
thermal core, 21,23,25,27	thermal core, 21,23,25,27	230 ± 3
thermal core, 21,23,25,27	fast core, 19	235 ± 14
fast core, 19	thermal core, 21,23,25,27	233 ± 4
fast core, 19	fast core, 19	195 ± 36